Lowest order constrained variational calculation for asymmetrical nuclear matter with the new Argonne potential

G. H. Bordbar and M. Modarres
Physics Department, Amir-Kabir University, Hafez Avenue, Tehran, Iran
and Centre for Theoretical Physics and Mathematics AEOI, P.O. Box 11365-8486, Tehran, Iran
(Received 17 June 1997)

The lowest order constrained variational method is used to calculate the properties of asymmetrical nuclear matter with the new charge-independent breaking, Argonne V_{18} (AV_{18}), as well as Argonne V_{14} (AV_{14}) potentials, for a wide range of density and proton to neutron ratio. The new AV_{18} potential, unlike AV_{14} and Δ-Reid interactions, overbinds nuclear matter at a saturation density of about 0.31 fm^{-3} which agrees well with the variational method based on hypernetted chain summation techniques. It is shown that it is not a good approximation to use the result of nuclear and neutron matter to get the equation of state of asymmetrical nuclear matter with an empirical parabolic approximation. Finally, various properties of asymmetrical nuclear matter such as incompressibility, symmetry energy, etc., are given and a comparison is made with the other many-body techniques. [S0556-2813(98)03501-8]

PACS number(s): 21.65.+f, 26.60.+c, 64.70.−p

I. INTRODUCTION

Since potential models which have fit only the np data often give a poor description of pp data [1], recently, a new nucleon-nucleon potential (AV_{18}) was proposed by Wiringa *et al.* [2]. This potential, which is an updated version of the Argonne V_{14} (AV_{14}) potential [3], is designed such that it fits both the pp and np data as well as low-energy nn scattering parameters and deuteron properties by using the Nijmegen NN scattering database [1,4]. Like the AV_{14} potential, it has been written in an operator format with a charge-independent part that has 14 operators (as before) and a charge-independent breaking part that has three charge-dependent and one charge-asymmetric operators. So in order to do nuclear many-body calculations with this potential one should treat explicitly the isospin projection in the nuclear many-body wave functions.

The lowest-order constrained variational (LOCV) which was developed by us several years ago [5–9] is a useful tool for the determination of the properties of nuclear matter. In the last years, the LOCV method has been extended further for finite temperature calculations and applied to neutron, nuclear, and asymmetrical nuclear matter [10–12]. In these LOCV calculations a nucleon-nucleon potential such as Reid soft core potential [13] (Reid) with inclusion of isobar degrees of freedom [5,14] (Δ-Reid) was used. Very recently we developed the LOCV method for V_8 [15], V_{12} [16], and Urbana V_{14} [16] potentials and we found similar results with respect to the other variational methods in which the many-body cluster contributions were included [17].

The LOCV method is a fully self-consistent formalism and it does not bring any free parameter into the calculation. It considers the normalization constraint to keep the higher order terms as small as possible [5,7] (this has been tested by calculating the three-body cluster terms; see [5,17]). The functional minimization procedure represents an enormous computational simplification over unconstrained methods (i.e., to parametrize the short-range behavior of correlation functions) that attempt to go beyond lowest order [15,21].

The equation of state of asymmetrical nuclear matter as well as its incompressibility plays an important role in the study of heavy-ion collisions [18], stellar collapse, supernova explosions, neutron stars, etc. [19]. Therefore, it is a great interest to predict such an equation of state by a full microscopic many-body calculation.

There are only a few microscopic calculations for asymmetrical nuclear matter [5,6,12,20]. In some of these calculations an empirical parabolic approximation has been used [21,22] (rather than an explicit calculation). So it is interesting to investigate the validity of this approximation at various proton fractions by performing a detailed calculation.

In the present work we intend to calculate the equation of state of asymmetrical nuclear matter by using the LOCV method with AV_{18} [2], AV_{14} [3], and Urbana V_{14} (UV_{14}) [16] potentials. So the plan of this article is as follows: The lowest-order constrained variational method is briefly described in Sec. II. Section III is devoted to results and a discussion for the binding energy (Sec. III A), symmetry energy (Sec. III B), and pressure and incompressibility (Sec. III C) of asymmetrical nuclear matter. Our summary and conclusions are presented in Sec. IV.

II. LOCV FORMALISM

We consider a trial many-body wave function of the form

$$\psi = F\phi, \tag{1}$$

where ϕ is a Slater determinant of plane waves of A independent nucleons, F is an A-body correlation operator which will be replaced by a Jastrow form, i.e.,

$$F = \mathcal{S}\prod_{i>j} f(ij), \tag{2}$$

and $\mathcal{S}$ is a symmetrizing operator. The cluster expansion of the energy functional is written as [23]

$$E([f])=\frac{1}{A}\frac{\langle\psi|H|\psi\rangle}{\langle\psi|\psi\rangle}=E_1+E_2+E_3+\cdots. \tag{3}$$

The one-body term E_1 for an asymmetrical nuclear matter that consists of Z protons and N neutrons is

$$E_1=\sum_{i=1,2}\frac{3}{5}\frac{\hbar^2k_i^{F^2}}{2m_i}\frac{\rho_i}{\rho}. \tag{4}$$

Labels 1 and 2 are used instead of proton and neutron, respectively, and $k_i^F=(3\pi^2\rho_i)^{1/3}$ is the Fermi momentum of particle i ($\rho=\rho_N+\rho_Z$).

The two-body energy E_2 is

$$E_2=\frac{1}{2A}\sum_{ij}\langle ij|\mathcal{V}(12)|ij-ji\rangle \tag{5}$$

and

$$\mathcal{V}(12)=-\frac{\hbar^2}{2m}[f(12),[\nabla_{12}^2,f(12)]]+f(12)V(12)f(12). \tag{6}$$

The two-body correlation operator $f(12)$ is defined as follows:

$$f(ij)=\sum_{\alpha,p=1}^{3}f_\alpha^{(p)}(ij)O_\alpha^{(p)}(ij). \tag{7}$$

$\alpha=\{J,L,S,T,T_z\}$ and the operators $O_\alpha^p(ij)$ are written as

$$O_\alpha^{p=1,3}=1,(\tfrac{2}{3}+\tfrac{1}{6}S_{12}),(\tfrac{1}{3}-\tfrac{1}{6}S_{12}), \tag{8}$$

where $S_{12}=3(\boldsymbol{\sigma}_1\cdot\hat{r})(\boldsymbol{\sigma}_2\cdot\hat{r})-\boldsymbol{\sigma}_1\cdot\boldsymbol{\sigma}_2$ is the tensor operator. We choose $p=1$ for uncoupled channels and $p=2,3$ for coupled channels.

The two-body nucleon-nucleon interaction $V(12)$ has the following form:

$$V(12)=\sum_{p=1}^{18}V^p(r_{12})O_{12}^p. \tag{9}$$

The first 14 operators are the same as before (see also our previous calculation with the UV_{14} potential [16]) and they are given by

$$\begin{aligned}O_{12}^{p=1-14}=&1,\boldsymbol{\sigma}_1\cdot\boldsymbol{\sigma}_2,\boldsymbol{\tau}_1\cdot\boldsymbol{\tau}_2,(\boldsymbol{\sigma}_1\cdot\boldsymbol{\sigma}_2)\\&\times(\boldsymbol{\tau}_1\cdot\boldsymbol{\tau}_2),S_{12},S_{12}(\boldsymbol{\tau}_1\cdot\boldsymbol{\tau}_2),\\&\mathbf{L}\cdot\mathbf{S},\mathbf{L}\cdot\mathbf{S}(\boldsymbol{\tau}_1\cdot\boldsymbol{\tau}_2),\mathbf{L}^2,\mathbf{L}^2(\boldsymbol{\sigma}_1\cdot\boldsymbol{\sigma}_2),\mathbf{L}^2(\boldsymbol{\tau}_1\cdot\boldsymbol{\tau}_2),\\&\mathbf{L}^2(\boldsymbol{\sigma}_1\cdot\boldsymbol{\sigma}_2)(\boldsymbol{\tau}_1\cdot\boldsymbol{\tau}_2),(\mathbf{L}\cdot\mathbf{S})^2,(\mathbf{L}\cdot\mathbf{S})^2(\boldsymbol{\tau}_1\cdot\boldsymbol{\tau}_2).\end{aligned} \tag{10}$$

The four additional operators which break charge independence are written as

$$O_{12}^{p=15-18}=\mathbf{T}_{12},(\boldsymbol{\sigma}_1\cdot\boldsymbol{\sigma}_2)\mathbf{T}_{12},S_{12}\mathbf{T}_{12},(\boldsymbol{\tau}_{z1}+\boldsymbol{\tau}_{z2}), \tag{11}$$

where $\mathbf{T}_{12}=3(\boldsymbol{\tau}_1\cdot\hat{r})(\boldsymbol{\tau}_2\cdot\hat{r})-\boldsymbol{\tau}_1\cdot\boldsymbol{\tau}_2$ is the isotensor operator. These 18 components are denoted by the labels c, $\boldsymbol{\sigma}$, $\boldsymbol{\tau}$, $\boldsymbol{\sigma\tau}$, t, $t\boldsymbol{\tau}$, ls, $ls\boldsymbol{\tau}$, $l2$, $l2\boldsymbol{\sigma}$, $l2\boldsymbol{\tau}$, $l2\boldsymbol{\sigma\tau}$, $ls2$, $ls2\boldsymbol{\tau}$, T, $\boldsymbol{\sigma}T$, tT, and $\boldsymbol{\tau z}$. The T, $\boldsymbol{\sigma}T$, and tT, operators are the charge-dependent forces, while the $\boldsymbol{\tau z}$ operator is the charge-asymmertic force [2]. By using correlation operators in the form of Eq. (7) and the two-nucleon potential from Eq. (9), we find the following equation for the two-body energy:

$$\begin{aligned}E_2=&\frac{2}{\pi^4\rho}\left(\frac{\hbar^2}{2m}\right)\sum_{JLSTT_z}(2J+1)\,\frac{1}{2}[1-(-1)^{L+S+T}]\left|\left\langle\frac{1}{2}\tau_{z1}\frac{1}{2}\tau_{z2}\middle|TT_z\right\rangle\right|^2\int dr\Bigg\{\Bigg[(f_\alpha^{(1)\prime})^2a_\alpha^{(1)^2}(k_Fr)+\frac{2m}{\hbar^2}(\{V_c-3V_\sigma+(V_\tau\\&-3V_{\sigma\tau})(4T-3)+(V_T-3V_{\sigma T})[T(6T_z^2-4)]+2V_{\tau z}T_z\}a_\alpha^{(1)^2}(k_Fr)+[V_{l2}-3V_{l2\sigma}+(V_{l2\tau}-3V_{l2\sigma\tau})(4T\\&-3)]c_\alpha^{(1)^2}(k_Fr))f_\alpha^{(1)^2}\Bigg]+\sum_{i=2,3}\Bigg[(f_\alpha^{(i)\prime})^2a_\alpha^{(i)^2}+\frac{2m}{\hbar^2}(\{V_c+V_\sigma+(-6i+14)V_t-(i-1)V_{ls}+[V_\tau+V_{\sigma\tau}+(-6i+14)V_{t\tau}\\&-(i-1)V_{ls\tau}](4T-3)+[V_T+V_{\sigma T}+(-6i+14)V_{tT}][T(6T_z^2-4)]+2V_{\tau z}T_z\}a_\alpha^{(i)^2}(k_Fr)+[V_{l2}+V_{l2\sigma}+(V_{l2\tau}+V_{l2\sigma\tau})\\&\times(4T-3)]c_\alpha^{(i)^2}(k_Fr)+[V_{ls2}+V_{ls2\tau}(4T-3)]d_\alpha^{(i)^2}(k_Fr))f_\alpha^{(i)^2}\Bigg]+\frac{2m}{\hbar^2}\Bigg\{V_{ls}-2V_{l2}-2V_{l2\sigma}-3V_{ls2}\\&+[(V_{ls\tau}-2V_{l2\tau}-2V_{l2\sigma\tau}-3V_{ls2\tau})(4T-3)]\}b_\alpha^2(k_Fr)f_\alpha^{(2)}f_\alpha^{(3)}+\frac{1}{r^2}(f_\alpha^{(2)}-f_\alpha^{(3)})^2b_\alpha^2(k_Fr)\Bigg\},\end{aligned} \tag{12}$$

where the coefficient $a_\alpha^{(1)^2}(x)$, etc., are defined as

$$a_\alpha^{(1)^2}(x)=x^2I_{L,T_z}(x), \tag{13}$$

$$a_\alpha^{(2)^2}(x)=x^2[\beta I_{J-1,T_z}(x)+\gamma I_{J+1,T_z}(x)], \tag{14}$$

$$a_\alpha^{(3)^2}(x)=x^2[\gamma I_{J-1,T_z}(x)+\beta I_{J+1,T_z}(x)], \tag{15}$$

$$b_\alpha^2(x)=x^2[\beta_{23}I_{J-1,T_z}(x)-\beta_{23}I_{J+1,T_z}(x)], \tag{16}$$

$$c_\alpha^{(1)^2}(x)=x^2\nu_1I_{L,T_z}(x), \tag{17}$$

$$c_\alpha^{(2)^2}(x)=x^2[\,\eta_2 I_{J-1,T_z}(x)+\nu_2 I_{J+1,T_z}(x)], \tag{18}$$

$$c_\alpha^{(3)^2}(x)=x^2[\,\eta_3 I_{J-1,T_z}(x)+\nu_3 I_{J+1,T_z}(x)], \tag{19}$$

$$d_\alpha^{(2)^2}(x)=x^2[\,\xi_2 I_{J-1,T_z}(x)+\lambda_2 I_{J+1,T_z}(x)], \tag{20}$$

$$d_\alpha^{(3)^2}(x)=x^2[\,\xi_3 I_{J-1,T_z}(x)+\lambda_3 I_{J+1,T_z}(x)], \tag{21}$$

with

$$\beta=\frac{J+1}{2J+1}, \tag{22}$$

$$\gamma=\frac{J}{2J+1}, \tag{23}$$

$$\beta_{23}=\frac{2J(J+1)}{2J+1}, \tag{24}$$

$$\nu_1=L(L+1), \tag{25}$$

$$\nu_2=\frac{J^2(J+1)}{2J+1}, \tag{26}$$

$$\nu_3=\frac{J^3+2J^2+3J+2}{2J+1}, \tag{27}$$

$$\eta_2=\frac{J(J^2+2J+1)}{2J+1}, \tag{28}$$

$$\eta_3=\frac{J(J^2+J+2)}{2J+1}, \tag{29}$$

$$\xi_2=\frac{J^3+2J^2+2J+1}{2J+1}, \tag{30}$$

$$\xi_3=\frac{J(J^2+J+4)}{2J+1}, \tag{31}$$

$$\lambda_2=\frac{J(J^2+J+1)}{2J+1}, \tag{32}$$

$$\lambda_3=\frac{J^3+2J^2+5J+4}{2J+1}, \tag{33}$$

and

$$I_{J,T_z}(x)=\int dq P_{T_z}(q) J_J^2(xq). \tag{34}$$

$P_{T_z}(q)$ is written as [τ_{z1} or $\tau_{z2}=-\frac{1}{2}$ (neutron) and $+\frac{1}{2}$ (proton)]

$$P_{T_z}(q)=\tfrac{2}{3}\pi[k_{\tau_{z1}}^{F^3}+k_{\tau_{z2}}^{F^3}-\tfrac{3}{2}(k_{\tau_{z1}}^{F^2}+k_{\tau_{z2}}^{F^2})q - \tfrac{3}{16}(k_{\tau_{z1}}^{F^2}-k_{\tau_{z2}}^{F^2})^2 q^{-1}+q^3] \tag{35}$$

for $\frac{1}{2}|k_{\tau_{z1}}^F-k_{\tau_{z2}}^F|<q<\frac{1}{2}|k_{\tau_{z1}}^F+k_{\tau_{z2}}^F|$,

$$P_{T_z}(q)=\tfrac{4}{3}\pi\ \min(k_{\tau_{z1}}^{F^3},k_{\tau_{z2}}^{F^3})$$

for $q<\frac{1}{2}|k_{\tau_{z1}}^F-k_{\tau_{z2}}^F|$, and

$$P_{T_z}(q)=0$$

for $q>\frac{1}{2}|k_{\tau_{z1}}^F+k_{\tau_{z2}}^F|$. The $J_J(x)$ are the familiar Bessel functions.

Now, we can minimize the two-body energy, Eq. (12), with respect to the variations in the functions $f_\alpha^{(i)}$ but subject to the normalization constraint [5,7]

$$\frac{1}{A}\sum_{ij}\langle ij|h_{T_z}^2(12)-f^2(12)|ij\rangle_a=0, \tag{36}$$

where in the case of asymmetrical nuclear matter the function $h_{T_z}(x)$ is defined as

$$h_{T_z}(r)=\left[1-\tfrac{9}{2}\left(\frac{J_1(k_i^F r)}{k_i^F r}\right)^2\right]^{-1/2} \quad (T_z=\pm 1) \qquad =1 \quad (T_z=0). \tag{37}$$

In terms of channel correlation functions we can write Eq. (36) as follows:

$$\frac{4}{\pi^4\rho}\sum_{\alpha,i}(2J+1)^{\frac{1}{2}}[1-(-1)^{L+S+T}]|\langle\tfrac{1}{2}\ \tau_{z1}\ \tfrac{1}{2}\ \tau_{z2}|TT_z\rangle|^2 \times\int_0^\infty dr[h_{T_z}^2(k_F r)-f_\alpha^{(i)^2}(r)]a_\alpha^{(i)^2}(k_F r)=0. \tag{38}$$

As we will see later, the above constraint introduces a Lagrange multiplier λ through which all of the correlation functions are coupled. From the minimization of the two-body cluster energy we get a set of coupled and uncoupled Euler-Lagrange differential equations. The Euler-Lagrange equations for uncoupled states are

$$g_\alpha^{(1)\prime\prime}-\left\{\frac{a_\alpha^{(1)\prime\prime}}{a_\alpha^{(1)}}+\frac{m}{\hbar^2}[V_c-3V_\sigma+(V_\tau-3V_{\sigma\tau})(4T-3)+(V_T -3V_{\sigma T})[T(6T_z^2-4)]+2V_{\tau z}T_z+\lambda]+\frac{m}{\hbar^2}[V_{l2}-3V_{l2\sigma} +(V_{l2\tau}-3V_{l2\sigma\tau})(4T-3)]\frac{c_\alpha^{(1)^2}}{a_\alpha^{(1)^2}}\right\}g_\alpha^{(1)}=0, \tag{39}$$

while the coupled equations are written as

$$g_\alpha^{(2)\prime\prime}-\left\{\frac{a_\alpha^{(2)\prime\prime}}{a_\alpha^{(2)}}+\frac{m}{\hbar^2}\{V_c+V_\sigma+2V_t-V_{ls}+(V_\tau+V_{\sigma\tau}+2V_{t\tau}-V_{ls\tau})(4T-3)+(V_T+V_{\sigma T}+2V_{tT})[T(6T_z^2-4)]+2V_{\tau z}T_z+\lambda\}+\frac{m}{\hbar^2}[V_{l2}+V_{l2\sigma}+(V_{l2\tau}+V_{l2\sigma\tau})(4T-3)]\frac{c_\alpha^{(2)^2}}{a_\alpha^{(2)^2}}+\frac{m}{\hbar^2}[V_{ls2}+V_{ls2\tau}(4T-3)]\frac{d_\alpha^{(2)^2}}{a_\alpha^{(2)^2}}+\frac{b_\alpha^2}{r^2a_\alpha^{(2)^2}}\right\}g_\alpha^{(2)}+\left\{\frac{1}{r^2}-\frac{m}{2\hbar^2}[V_{ls}-2V_{l2}-2V_{l2\sigma}-3V_{ls2}+(V_{ls\tau}-2V_{l2\tau}-2V_{l2\sigma\tau}-3V_{ls2\tau})(4T-3)]\right\}\frac{b_\alpha^2}{a_\alpha^{(2)}a_\alpha^{(3)}}g_\alpha^{(3)}=0, \tag{40}$$

$$g_\alpha^{(3)\prime\prime}-\left\{\frac{a_\alpha^{(3)\prime\prime}}{a_\alpha^{(3)}}+\frac{m}{\hbar^2}\{V_c+V_\sigma-4V_t-2V_{ls}+(V_\tau+V_{\sigma\tau}-4V_{t\tau}-2V_{ls\tau})(4T-3)+(V_T+V_{\sigma T}-4V_{tT})[T(6T_z^2-4)]+2V_{\tau z}T_z+\lambda\}+\frac{m}{\hbar^2}[V_{l2}+V_{l2\sigma}+(V_{l2\tau}+V_{l2\sigma\tau})(4T-3)]\frac{c_\alpha^{(3)^2}}{a_\alpha^{(3)^2}}+\frac{m}{\hbar^2}[V_{ls2}+V_{ls2\tau}(4T-3)]\frac{d_\alpha^{(3)^2}}{a_\alpha^{(3)^2}}+\frac{b_\alpha^2}{r^2a_\alpha^{(2)^2}}\right\}g_\alpha^{(3)}+\left\{\frac{1}{r^2}-\frac{m}{2\hbar^2}[V_{ls}-2V_{l2}-2V_{l2\sigma}-3V_{ls2}+(V_{ls\tau}-2V_{l2\tau}-2V_{l2\sigma\tau}-3V_{ls2\tau})(4T-3)]\right\}\frac{b_\alpha^2}{a_\alpha^{(2)}a_\alpha^{(3)}}g_\alpha^{(2)}=0, \tag{41}$$

where

$$g_\alpha^{(i)}(r)=f_\alpha^{(i)}(r)a_\alpha^{(i)}(r). \tag{42}$$

The primes in the above equations mean differentiation with respect to r. As we pointed out before, the Lagrange multiplier λ is associated with the normalization constraint, Eq. (38). The constraint is incorporated by solving the Euler-Lagrange equations only out to certain distances, until the logarithmic derivative of the correlation functions matches those of $h_{T_z}(r)$ and then we set the correlation functions equal to $h_{T_z}(r)$ (beyond these state-dependence healing distances).

III. RESULTS AND DISCUSSION

A. Binding energy

In Fig. 1 we have plotted the result of our binding energy calculation for asymmetrical nuclear matter with the AV_{18} and the AV_{14} potentials for different values of the proton to

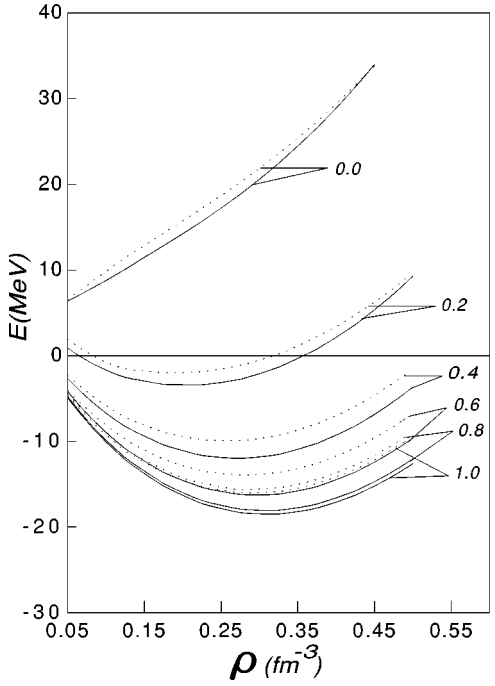

FIG. 1. The binding energy of asymmetrical nuclear matter versus density for various proton to neutron ratios ($\mathcal{R}$). Dotted curve for AV_{14} and solid curve for AV_{18} potentials.

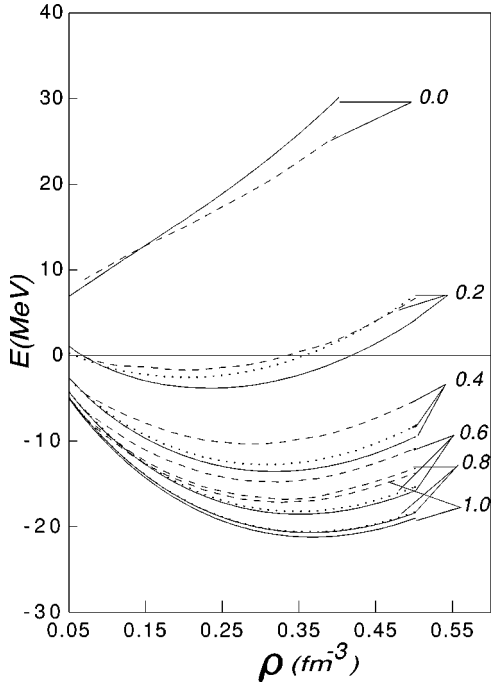

FIG. 2. As in Fig. 1 but for the UV_{14} potential. Exact LOCV calculation (solid curve) and approximate LOCV calculation (dotted curve). WFF results [21] (dashed curve).

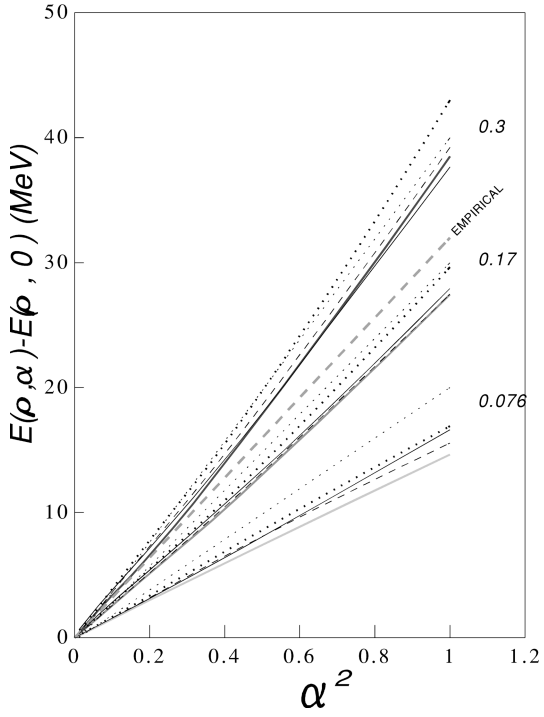

FIG. 3. Quadratic dependence of asymmetric energy for different potentials: Δ-Reid (solid curve), AV_{14} (light solid curve), AV_{18} (dashed curve), and UV_{14} (heavy dotted curve). Dotted curve is the result of BL [20].

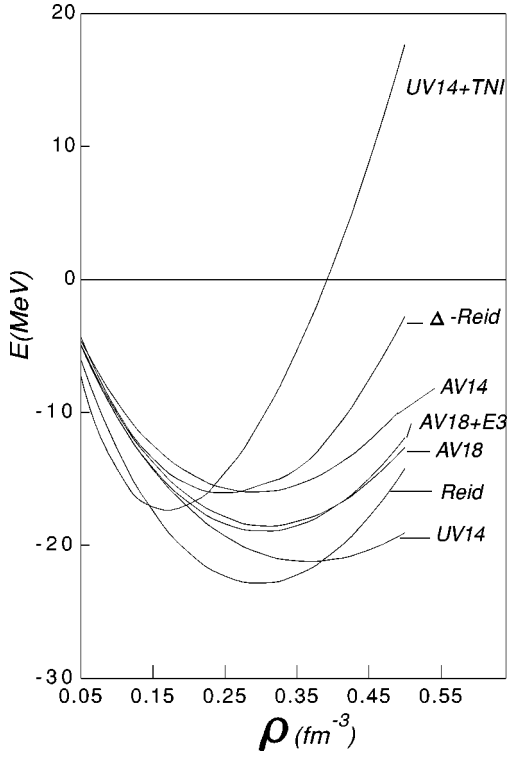

FIG. 4. The binding energy of nuclear matter versus density for different potentials.

neutron ratio ($\mathcal{R}=0.0$, 0.2, 0.4, 0.6, 0.8, 1.0) versus density. This figure shows that as we increase $\mathcal{R}$ the AV_{18} potential gives more binding energy than the AV_{14} potential. So we can conclude that at high values of the density, $T=0$ channels give more attraction for the AV_{18} than the AV_{14} potentials. It is seen that the AV_{18} potential overbinds nuclear matter ($\mathcal{R}=1.0$) while the AV_{14} potential reproduces the correct binding. But their saturation densities are far from empirical nuclear matter value ($0.17\ \mathrm{fm}^{-3}$). As we pointed out before, in some of the works [21,22], the asymmetrical nuclear matter binding energy has been calculated by using the results of many-body calculations for two extreme situations, namely, nuclear ($\mathcal{R}=1.0$) and neutron ($\mathcal{R}=0.0$) matter with a parabolic approximation, i.e.,

$$E_{\mathrm{approx}}(\rho,\alpha)=E_{\mathrm{nuclear}}(\rho,\alpha=0)+E_{\mathrm{sym}}(\rho)\alpha^2, \qquad (43)$$

where the asymmetry parameter is $\alpha=(1-\mathcal{R})/(1+\mathcal{R})$ and symmetry energy is

$$E_{\mathrm{sym}}=E_{\mathrm{neutron}}(\alpha=1)-E_{\mathrm{nuclear}}(\alpha=0). \qquad (44)$$

TABLE I. The saturation energy and density of nuclear matter as well as its incompressibility for different potentials and many-body methods.

Potential	Method	Author	ρ_0 (fm^{-3})	E(ρ_0) (MeV)	$\mathcal{K}$ (MeV)
AV_{18}	LOCV	BM	0.310	−18.46	302
AV_{14}	LOCV	BM	0.290	−15.99	248
	Variational	WFF [21]	0.319	−15.60	205
	BB	DW [24]	0.280	−17.80	247
	BHF	BBB [25]	0.256	−18.26	—
UV_{14}	LOCV	BM	0.366	−21.20	311
	Variational	CP [26]	0.349	−20.00	—
	Variational	WFF [21]	0.326	−17.10	243
UV_{14}+TNI	LOCV	BM	0.170	−17.33	276
	Variational	WFF [21]	0.157	−16.60	261
	CBF	FFP [27]	0.163	−18.30	269
Δ-Reid	LOCV	MI [5]	0.258	−16.28	300
Reid	LOCV	HBI [6]	0.294	−22.83	340
	LOCV	MO [28]	0.230	−14.58	238
Empirical			0.170	−15.86	(200–300)

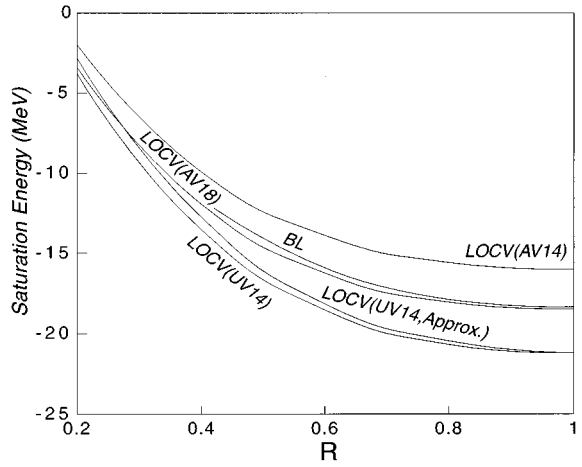

FIG. 5. The saturation energy of asymmetrical nuclear matter versus proton to neutron ratio ($\mathcal{R}$).

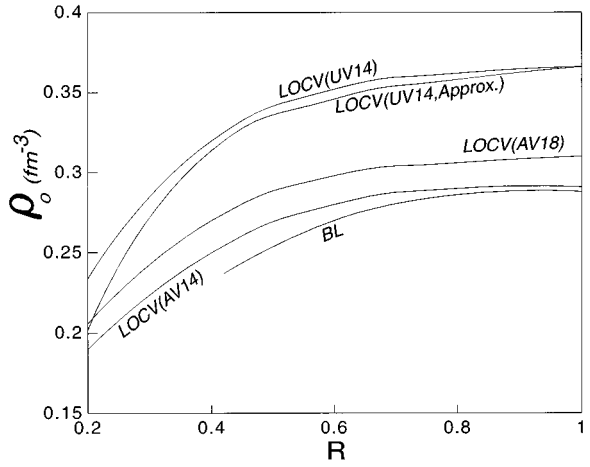

FIG. 6. As in Fig. 5 but for the saturation density.

Our approximation results and those of Wiringa, Ficks, and Fabrocini (WFF) [21] together with the explicit LOCV microscopic calculations with the UV_{14} potential are displayed in Fig. 2. As one expects, this approximation should only be valid for small values of α (large $\mathcal{R}$). This feature can be clearly seen from this figure.

In Fig. 3, we compare the quadratic dependence (α^2) of our asymmetry energy results [i.e., $E(\rho,\alpha)-E(\rho,0)$] for different potentials with those of Bombaci and Lombardo (BL) [20] at different densities, i.e., 0.076, 0.17, and 0.3 fm^{-3}. It is seen that at higher values of α we cannot exactly fullfill the parabolic approximation. But in general we are close to the empirical value at nuclear matter saturation density. The results with the UV_{14} potential are much closer to the empirical value than the others.

Figure 4 shows the comparison of nuclear matter binding energies for different potentials. The saturation curve with the AV_{14} and the Δ-Reid potentials is closer to the empirical prediction with respect to the other potentials [without a three-nucleon interaction (TNI)]. Even the enclosion of three-body cluster terms [5,17] and the three-nucleon potential [16] cannot predict the empirical values exactly with the AV_{18} and the UV_{14} potentials, respectively. However, the results of UV_{14}+TNI is much better with respect to the other calculations.

In Table I we give our saturation energy and saturation density of nuclear matter calculations for different potentials. The results of the others calculations are also given for comparison. The difference between our LOCV calculation and those of Mittet and Ostgaard (MO) [28] has been discussed in Ref. [17]. Again it is seen that only results of the AV_{14} and the Δ-Reid potentials are close to the empirical values given in this table and the inclusion of the TNI improves the calculation.

In Fig. 5 we plot the saturation energy of asymmetrical nuclear matter versus the proton to neutron ratio $\mathcal{R}$ for various potentials. The result of BL [20] is also given for comparison. Again, it is clearly seen that as we reach small values of $\mathcal{R}(\simeq 0.2)$ the difference between exact and approximated calculations (for the UV_{14} potential) becomes sizable. But for very small values of $\mathcal{R}(\simeq 0.0)$ again the difference becomes negligible. The same comparison is given for the saturation density against ratio $\mathcal{R}$ in Fig. 6. We get similar results to those of BL [20] with the AV_{14} potential. This result is in agreement with what BL [20] have pointed out, that the Paris and the AV_{14} potentials are very similar to each other.

When this manuscript was in preparation, we obtained a preprint from Akmal and Pandharipande [29]. They have performed the variational method based on hypernetted chain summation (VCS) techniques with the AV_{18} potential. They have given only the nuclear matter energies -14.71 and -18.37 MeV at two values of nuclear matter density $\rho = 0.16$ and 0.28 fm^{-3}, respectively. These values can be compared with our LOCV calculation for the AV_{18} potential in Fig. 1 [the exact figures are $E(0.16\ \text{fm}^{-3})=-14.47$ MeV and $E(0.28\ \text{fm}^{-3})=-18.34$ MeV) which is surprisingly close to the Akmal-Pandharipande calculations [29].

B. Symmetry energy

In general the symmetry energy is defined as

$$E_{\text{sym}}(\rho)=\frac{1}{2}\left.\frac{\partial^2 E(\rho,\alpha)}{\partial\alpha^2}\right|_{\alpha=0}. \tag{45}$$

But it is also possible to make an approximation and use Eq. (44). The result is displayed in Fig. 7 for various potentials [according to Eq. (45)]. It is seen that the calculation of WFF

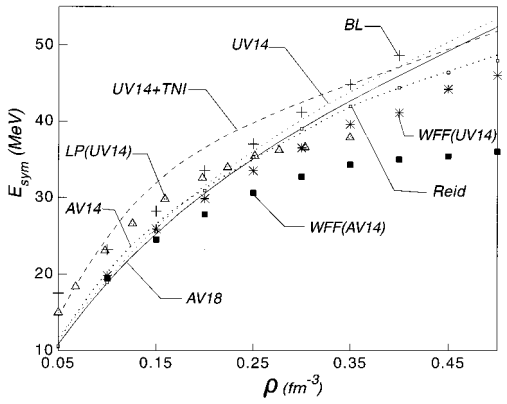

FIG. 7. The symmetry energy versus density for different potentials and methods.

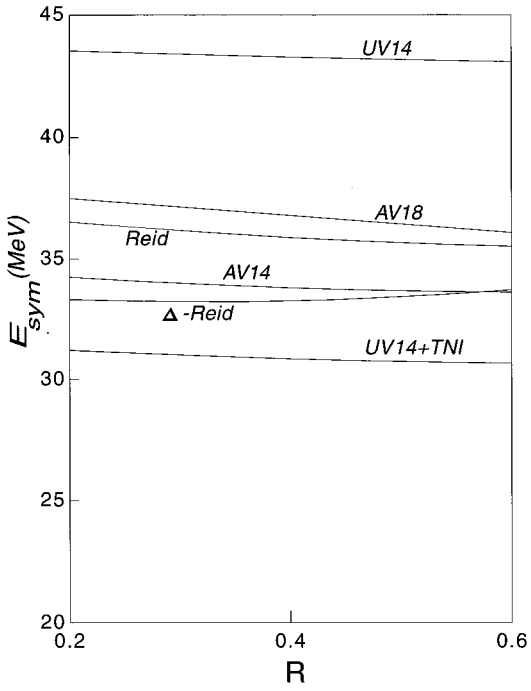

FIG. 8. As in Fig. 7 but for the proton to neutron ratio ($\mathcal{R}$).

[21] in which the $E_{\rm sym}(\rho)$ has been evaluated by using Eq. (44) differs from the other calculations. Our results with the AV_{18} and the AV_{14} potentials are in agreement with those of BL [20].

The ratio ($\mathcal{R}$) dependence of symmetry energies for various potentials at their saturation densities (symmetry coefficient) is given in Fig. 8. From the semiempirical mass formula, this should vary between 28 to 32 MeV [25]. It is seen that only the AV_{14}, the Δ-Reid, and the UV_{14}+TNI potentials give values near the empirical prediction.

C. Pressure and incompressibility

By differentiating asymmetrical nuclear matter saturation curve at each ratio ($\mathcal{R}$) with respect to the density we can evaluate the corresponding pressure,

$$P=\rho^2\left(\frac{\partial E(\rho,\mathcal{R})}{\partial\rho}\right)_{\mathcal{R}}. \tag{46}$$

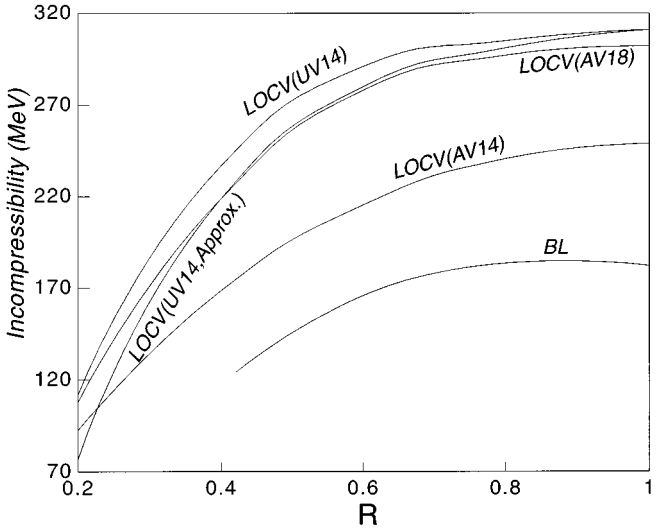

FIG. 9. As Fig. 5 but for incompressibility.

The results are displayed in Table II for two values of $\mathcal{R}=0.8$ and 0.2 with the AV_{18}, AV_{14}, and the UV_{14} potentials. The approximated pressure using Eq. (43) and the UV_{14} potential is also displayed. The difference between the exact and the approximation calculations becomes more sizable, especially for smaller ratios.

In the last row of Table I, we give the incompressibility of symmetrical nuclear matter ($\alpha=0$) for various potentials, i.e.,

$$\mathcal{K}(\alpha)=9\rho_0^2(\alpha)\left.\frac{\partial^2E(\rho,\alpha)}{\partial\rho^2}\right|_{\rho_0(\alpha)}. \tag{47}$$

The other results as well as the experimental prediction [30] are also given for comparison. Figure 9 shows the asymmetrical incompressibility as a function of $\mathcal{R}$. The result of BL [20] is also displayed. UV_{14} (approx.) is the result of incompressibility calculations, using only two extreme situations, namely, neutron and nuclear matter.

IV. SUMMARY AND CONCLUSION

We have computed the equation of state of asymmetrical nuclear matter and some of its properties such as symmetry

TABLE II. The pressure of asymmetrical nuclear matter.

	$\mathcal{R}=0.8$				$\mathcal{R}=0.2$			
ρ	AV_{18}	AV_{14}	UV_{14}	UV_{14} (approx.)	AV_{18}	AV_{14}	UV_{14}	UV_{14} (approx.)
0.05	−0.299	−0.229	−0.305	−0.261	−0.170	−0.037	−0.168	−0.084
0.1	−0.855	−0.728	−0.896	−0.821	−0.364	−0.213	−0.398	−0.219
0.15	−1.357	−1.160	−1.500	−1.414	−0.366	−0.267	−0.474	−0.223
0.2	−1.578	−1.246	−1.933	−1.799	−0.039	0.084	−0.318	0.036
0.25	−1.288	−0.803	−2.014	−1.781	0.812	0.964	0.226	0.713
0.3	−0.238	0.316	−1.558	−1.286	2.484	2.434	1.345	1.979
0.35	1.769	2.294	−0.328	−0.149	5.202	4.682	3.205	4.034
0.4	4.890	5.372	1.457	1.858	9.146	8.106	5.910	7.065

energy, pressure, etc. Several two-body potentials as well as the new AV_{18} potential have been used in order to test the N-N interactions and various many-body techniques against each other. A full microscopic calculation has been presented which enabled us to check the validity of different empirical values. It is found that the asymmetrical nuclear matter binding energy is in good agreement with the empirical mass formula. But it is not a good approximation to use the neutron and nuclear matter results to get an equation of state of asymmetrical nuclear matter, especially at small proton to neutron ratios. This is very important when one intends to calculate the pressure and incompressibility of nucleonic matter.

It was shown that the new AV_{18} potential does overbind nuclear matter and a very good agreement was found between the LOCV result and more sophisticated approaches like Brueckner-Hartree-Fock (BHF) and variational hypernetted chain techniques.

[1] V. G. J. Stoks and J. J. de Swart, Phys. Rev. C **47**, 761 (1993).
[2] R. B. Wiringa, V. Stoks, and R. Schiavilla, Phys. Rev. C **51**, 38 (1995).
[3] R. B. Wiringa, R. A. Smith, and T. L. Ainsworth, Phys. Rev. C **29**, 1207 (1984).
[4] J. R. Bergevoet, P. C. Van Campen, R. A. M. Klomp, J. L. de Kok, T. A. Rijken, V. G. J. Stoks, and J. J. de Swart, Phys. Rev. C **41**, 1435 (1990); V. G. J. Stoks, R. A. M. Klomp, M. C. M. Rentsmeeter, and J. J. de Swart, Phys. Rev. C **48**, 792 (1993).
[5] M. Modarres and J. M. Irvine, J. Phys. G **5**, 511 (1979); **5**, 7 (1979).
[6] C. Howes, R. F. Bishop, and J. M. Irvine, J. Phys. G **4**, 89 (1978); **4**, 11 (1979).
[7] J. C. Owen, R. F. Bishop, and J. M. Irvine, Nucl. Phys. **A277**, 45 (1977).
[8] C. Howes, R. F. Bishop, and J. M. Irvine, J. Phys. G **4**, 123 (1978).
[9] R. F. Bishop, C. Howes, J. M. Irvine, and M. Modarres, J. Phys. G **4**, 1709 (1978).
[10] M. Modarres, J. Phys. G **19**, 1349 (1993).
[11] M. Modarres, J. Phys. G **21**, 351 (1995).
[12] M. Modarres, J. Phys. G **23**, 923 (1997).
[13] R. V. Reid, Ann. Phys. (N.Y.) **50**, 411 (1968).
[14] A. M. Green, J. A. Niskanen, and M. E. Sainio, J. Phys. G **4**, 1085 (1978).
[15] I. E. Lagaris and V. R. Pandharipande, Nucl. Phys. **A334**, 217 (1980).
[16] I. E. Lagaris and V. R. Pandharipande, Nucl. Phys. **A359**, 331 (1981).
[17] G. H. Bordbar and M. Modarres, J. Phys. G **23**, 1631 (1997).
[18] R. Stoch *et al.*, Phys. Rev. Lett. **49**, 1236 (1982); J. J. Molitoris, D. Hahn, and H. Stocker, Nucl. Phys. **A447**, 13c (1985); H. Stocker and W. Greiner, Phys. Rep. **137**, 137 (1986); G. F. Bertsch and S. Das Gupta, *ibid.* **160**, 189 (1988).
[19] J. M. Lattimer, C. J. Pethick, M. Prakash, and P. Hansel, Phys. Rev. Lett. **66**, 2701 (1991); M. Prakash, I. Bombaci, P. J. Ellis, R. Knorren, and J. M. Lattimer, Phys. Rep. **280**, 1 (1997).
[20] I. Bombaci and U. Lombardo, Phys. Rev. C **44**, 1892 (1991).
[21] R. B. Wiringa, V. Ficks, and A. Fabrocini, Phys. Rev. C **38**, 1010 (1988).
[22] I. E. Lagaris and V. R. Pandharipande, Nucl. Phys. **A369**, 470 (1981).
[23] J. W. Clark, Prog. Part. Nucl. Phys. **2**, 89 (1979).
[24] B. D. Day and R. B. Wiringa, Phys. Rev. C **32**, 1057 (1985).
[25] M. Baldo, I. Bombaci, and G. F. Burgio, Astron. Astrophys. (to be published).
[26] J. Carlson and V. R. Pandharipande, Nucl. Phys. **A401**, 821 (1981).
[27] S. Fantoni, B. L. Friman, and V. R. Pandharipande, Nucl. Phys. **A399**, 51 (1983).
[28] R. Mittet and E. Ostgaard, Nucl. Phys. **A470**, 161 (1983).
[29] A. Akmal and V. R. Pandharipande, nucl-th/9705013.
[30] W. D. Myers and W. J. Swiatecky, Nucl. Phys. **A601**, 141 (1996).